www.vbripress.com, www.amlett.com, DOI: 10.5185/amlett.2011.11318 Published online by the VBRI Press in 2012

Synthesis of nanostructured iron-antimonate and its application in liquefied petroleum gas sensor

Satyendra Singh[1], B. C. Yadav[1,2*], Archana Singh[1], Prabhat K. Dwivedi[3]

[1]*Nanomaterials and Sensors Research Laboratory, Department of Physics, University of Lucknow, Lucknow 226007, U.P., India*

[2]*Department of Applied Physics, School for Physical Sciences, Babasaheb Bhimrao Ambedkar University, Lucknow 226025, U.P., India*

[3]*DST Unit on Nanosciences, Department of Chemical Engineering, Indian Institute of Technology Kanpur, Kanpur, U.P., India*

*Corresponding author. Tel: (+91) 9450094590 ; E-mail: balchandra_yadav@rediffmail.com

Received: 13 November 2011, Revised: 05 February 2012 and Accepted: 13 February 2012

ABSTRACT

In this paper we report the synthesis of iron-antimonate ($FeSbO_4$) via co-precipitation method for the LPG sensing application. X-ray diffraction (XRD), Scanning electron microscopy (SEM) and Energy dispersive X-ray analysis (EDAX) were used to confirm the crystal structure, crystallite size, surface morphology and elemental composition of the sensing material. Our XRD results confirm the single phase formation with tetragonal crystal structure of the synthesized material. Extremely broad reflections were observed indicating nanosized particle nature of the material obtained. The estimated value of average crystallite size was found 3 nm. Optical characterizations were done using UV-visible spectrophotometer and the value of energy band gap was found 3.8 eV by Tauc plot. Fine powder resulted from the chemical co-precipitation reaction was used to prepare the LPG sensing element in the form of pellet. The average sensor response of the $FeSbO_4$ pellet was 2.2. LPG sensor based on iron-antimonate shows 97% reproducibility after one month, which illustrates the stability of the fabricated sensor. Electrical properties of iron-antimonate in air were also investigated. Copyright © 2012 VBRI Press.

Keywords: Iron-antimonate; surface morphology; chemical co-precipitation; LPG sensor.

Satyendra Singh has received his B.Sc. and M.Sc. degrees in 2005 and 2007 respectively from University of Lucknow, Lucknow, Uttar Pradesh, India. Currently he is a Senior Research Fellow in Department of Physics, University of Lucknow, Lucknow and doing his Ph.D. under the supervision of Dr. B.C. Yadav, of the same university. His research topic is "Synthesis and Characterization of Nanostructured Semiconducting oxides and their Applications in Gas Sensor".

B.C. Yadav has received his B.Sc. and M.Sc. Degrees from Dr. R.M.L. Avadh University, Faizabad, U.P., India in the years 1991 and 1993 respectively. He obtained his Ph.D. degree in year 2001 from Department of Physics, University of Lucknow, India and selected as Associate Professor in Department of Applied Physics, School for Physical Sciences, Babasaheb Bhimrao Ambedkar University, Lucknow, U.P., India. Also he is working as Principal Investigator on various science and technology projects. He is recipient of prestigious Young Scientist Award-2005 instituted by CST. Currently he has been selected as International Fellow under Brain-Pool Program of KOFST, South Korea. His current interests of research are synthesis of nanomaterials and their applications as sensors.

Archana Singh has received her B.Sc. and M.Sc. degrees in 2008 and 2010 respectively from University of Lucknow, Lucknow, Uttar Pradesh, India. Currently he is doing Ph.D. in Department of Physics, University of Lucknow, Lucknow. Her area of interest is "Synthesis and Characterization of Polymer assisted nanostructured semiconducting oxides as Gas Sensors".

Prabhat K. Dwivedi is an experimental physicist. He received his Ph.D. from the Harcourt Butler Technological Institute, Kanpur. He has been a Visiting Researcher at the University of Alberta/TRLabs, Edmonton, Canada before joining DST unit on Nanosciences at IIT Kanpur. His main research interest lies in optical properties of photonic materials, Micro-and nanomechanical systems and development of micro/nanofabrication infrastructure. Currently, he is working on fabrication of 3-D structures on different materials using gray scale lithography.

Introduction

Ferric oxide is a well known magnetic material for the various applications. In recent years chemical sensors based on ferric oxide and its nanocomposites have been reported for their gas sensing properties [**1-9**]. Therefore, the synthesis of ferric oxide and its nanocomposites have received much attention in recent years [**10-14**]. The ultra fine particles of ferric oxides are found to alter the electrical properties on the chemical interaction with various gases, which is essential requirement for gas sensing applications [**15**]. Therefore, new synthetic routes for the preparation of Fe_2O_3 are being continuously investigated. Conventionally, γ-Fe_2O_3 powders with monodispersed particles are synthesized first by means of forced hydrolysis of ferric nitrate or ferric chloride in aqueous solutions, which produces α-Fe_2O_3 and then it is transformed into γ-Fe_2O_3 under a high-temperature process. To effectively control the particle shape and size, which is essential for achieving the desired sensing properties, the hydrolysis solution must be very dilute [**16-17**]. Gopal Reddy et al have reported the synthesis of γ-Fe_2O_3 for sensor application through a novel technique of combustion of ferric salts with hydrazine hydrate [**18**]. They have also reported that the γ-Fe_2O_3 and the Pt dispersed γ-Fe_2O_3 samples prepared through this process can be effectively used as materials for gas sensors. However, these kinds of gas sensors have low sensitivity, though the sensitivity can be enhanced to some extent by the proper choice of operating temperature or chemical modification [**19-22**].
LPG sensing at room temperature is interesting for industrial applications as most of the currently available LPG sensors are operated above room temperature [**23-26**]. Since room temperature LPG sensing is considered to be very effective for the commercial sensor point of view, hence in order to enhance the sensitivity, ferric oxide was chemically modified and mixed oxides were formed. The additives formed the new phases or binary compounds which will influence the size and surface morphology of the ferric oxide and hence modify the properties of that. Therefore, they are able to change the sensitivity, selectivity and response of ferric oxide based sensor. SbO_2 can modify the intrinsic physical properties of Fe_2O_3, such as: a) the electrical transport properties by introduction of new states in the band structure of Fe_2O_3; b) the surface morphology, which has an important role in the chemical reactions between oxide and gas; c) the grain size distribution, which contributes in determining the electrical resistance of the material and also the antimony used as a catalyst.

The $FeSbO_4$ structure is described in terms of a rutile-like framework with Fe and Sb cations distributed in the octahedral sites within the oxygen lattice [**27**]. Iron-antimonate is a model catalyst for the selective oxidation of hydrocarbons and an important component of some of the industrial catalyst for these reactions [**28**]. From catalytic properties point of view, iron-antimonate belongs to a family of oxidation catalysts in which the oxygen is taken from the catalyst surface, which is then re-oxidized by the oxygen in the gas phase. Therefore, in present investigation a special attention was focused on $FeSbO_4$ in order to obtain reliable gas sensors operable at room temperature.

The interaction between the gas molecules and the surface of the sensing element depends on its surface morphological structure and microstructure [**7, 29**]. If the surface of sensing material is porous then the LPG easily adsorb on its surface and diffuses through pores. After exposure, it gives sufficient changes in the electrical response of the material. The LPG sensing mechanism of such type of sensor involves the chemisorptions of oxygen on the surface of material, followed by charge transfer during the reaction of oxygen with LPG molecules, which will cause a change in resistance on the surface of a sensor [**30**]. If on interaction with the gas to the material, a much more variation is observed in the resistance then that sensing material is considered more sensitive to the particular gas. This property of nanosized material has been utilized for detection of gases.

Some of groups have fabricated nano grain sized ZnO and tested it for gas sensitivity. Dong et al [**31**] prepared nanosized ZnO prepared by the arc plasma method and showed that nano-ZnO exhibits the higher sensitivity compared to coarse-grained ZnO and lower operating temperatures (200-300 °C). The nano-ZnO exhibited higher sensitivities towards LPG and C_2H_2 then to H_2 and CO, and nano-ZnO with Fe and Ag additives showed high sensitivity and excellent selectivity to H_2 against C_2H_2, CO and LPG and with the response time less than 15 sec at 150 °C. Xu et al [**32**] also investigated the grain size effects on the sensor responses to the H_2, C_4H_{10} and C_2H_5OH. It is reported that smaller grain size of pure ZnO has higher gas sensitivity. The effect of film thickness on sensor performance was investigated by Chang et al. [**33**]. They fabricated ZnO films using r. f. reactive sputtering on a SiO_2/Si wafer with variable thickness (65 nm to 390 nm). The best sensitivity and faster response were obtained with the thin film (65 nm). Gopal Reddy et al. studied the ferrites prepared by wet chemical precipitation as gas sensing materials. They reported the response of zinc ferrite for H_2S and that of nickel ferrite for Cl_2. Tianshua et al. reported the response of cadmium ferrite for ethanol sensor [**34**]. Currently it is a topic of increasing interest to study the gas sensing properties of ferrites [**4-9**].

The main goal of our present investigation is to design and fabricate a LPG sensor which would be robust, cheap and more sensitive than previous reported sensors [**35-39**]. This investigation may be considered as the next step from our previous work in view of enhancement of sensitivity of LPG sensor. Besides this, we have also investigated the microstructure and optical characteristics of iron-antimonate in order to understand the advancement of fascinating LPG sensing properties.

Experimental

Iron-antimonate was synthesized by chemical co-precipitation method using ferric and antimony chlorides as a starting materials. All reagents were purchased from Merck, India and were of analytical grades (99% pure) which were used without further purification. 1 M solution of ferric chloride and antimony chloride were made by dissolving these in to required amount of absolute ethanol. These solutions were constant stirred for 6 h at 50ºC. After that both solutions were properly mixed in 3:1 molar ratios

and the obtained solution was refluxed at 50°C for 6 h in a rotary vacuum evaporator. The resulting solution was precipitated by using a drop wise addition of base agent (ammonium hydroxide) under continuous stirring to achieve simultaneous precipitation of both iron and antimony hydroxides. The chemical reaction that took place is as follows:

$$\text{Ethanolic solution of } (FeCl_3 + SbCl_3) \xrightarrow[\text{dropwise addition}]{NH_4OH} \text{ppt. of Fe and Sb hydroxides}$$

For the formation of crystalline powder, the precipitate of ferric and antimony hydroxides was repeatedly washed with deionized water and then dried at 80ºC for 4 h. Then obtained powder was annealed at 450ºC for 2 h. The following chemical reaction is assumed to occur during the co-precipitation of $FeSbO_4$ powder:

$$2Sb(OH)_3 + 2Fe(OH)_3 + O_2 \xrightarrow{450^\circ C} 2FeSbO_4 + 6H_2O$$

The crystalline powder after phase formation at 450ºC was crushed into fine powder using mortar and pestle. Sensing pellet of this co-precipitated powder was made by using hydraulic press (MB instruments, Delhi) under a uniaxial pressure of 616 MPa. The pellet was 9 mm in diameter and 3 mm in thickness.

For the gas sensing measurements, the sensing pellet with silver contacts was placed within a specially designed gas chamber having gas inlet and an outlet. Now this was exposed with the LPG and the variations in electrical resistance of the sensing material with the time due to the chemical surface interaction were recorded by using a Keithley electrometer (Model 6514). Gas sensitive properties of sensing elements were measured for different vol.% of LPG. The sensitivity (sensor speed) of sensing element is defined as the slope of the resistance-time curve and is given below [**35**]:

$$S = \Delta R / \Delta t$$

The sensitivity of the sensor is to be high due to adequate change in resistance (ΔR) in a minute time (Δt) in the presence of LPG, and for an enhanced performance it is desired that both the changes occur accordingly. If more changes are found in electrical resistance of the sensing material under consideration, the more will be the sensitivity of the sensor. Percentage sensor response for the sensing material is defined as [**35**]:

$$\%S.R. = \frac{|R_a - R_g|}{R_a} * 100$$

where R_a and R_g are the resistance values of the sensor in air and gas-air mixture, respectively.

For measuring the electrical properties of the sensing pellet in air, the pellet was put inside a tubular furnace at the highest point of temperature profile with electrical connections and variations in electrical resistance with temperature were recorded. The used heating rate was about 2 ºC per minute.

Scanning electron microscopy and energy dispersive X-ray analysis

The surface morphology of the sensing pellet was analyzed by scanning electron microscope (SEM, LEO-0430 Cambridge) coupled with EDAX. **Fig. 1a** and **b** show the surface morphology of sensing pellet before and after exposing to LPG, respectively. **Fig. 1a** shows that the particles are mostly irregular in shape and some particles are found as agglomerated and leaving some spaces as pores. These pores serve as gas adsorption sites and gas sensitivity depends on the size of the pores. Since sensing surfaces has dangling bonds, therefore the surface can be chemically very reactive. Owing to this reactivity when we expose LPG at the surface of sensing pellet then the gas diffuses through the pores wherein reaction of LPG with material surface occurs. Therefore, when the LPG is adsorbed on the surface of sensing pellet, it reduces the size of pores which can be seen from **Fig. 1b**.

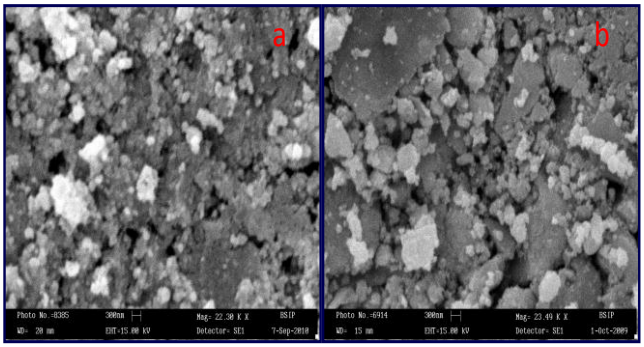

Fig. 1. SEM image of sensing pellet: **(a)** before exposing to LPG, **(b)** after exposing to LPG.

Energy dispersive X-ray spectroscopy was used for identifying the elemental compositions of the synthesized powder. The EDAX spectrum is shown in **Fig. 2** with reference to peak at 0 KeV. Spectrum indicates the presence of antimony, iron, oxygen, gold and carbon elements in the compound with 7.20, 20.47, 64.45, 0.99 and 6.89 atomic weight percentages respectively.

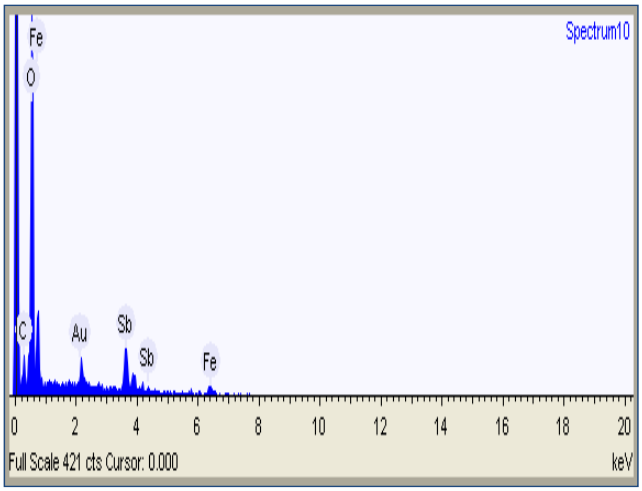

Fig. 2. EDAX of $FeSbO_4$ pellet.

Density and porosity analysis

Porosity of the sensing pellet was calculated by the relation [**40**]:

$$P = 1 - \frac{d}{d_x}$$

where $d = m/V$; determined from dimensions and mass of the pellet, and d_x is the X-ray density of the sample which have been calculated from the values of lattice parameters using the formula [**41, 42**]:

$$d_x = \frac{2M}{Na^3}$$

where the factor '2' represents the number of molecules in a unit cell of a tetragonal crystal structure, 'M' the molecular weight of the sample, 'N' the Avogadro number and 'a' the lattice parameter of the sample. Our analysis shows that the surface of sensing pellet is 46% porous which enables larger specific surface area for the adsorption of LPG to react yielding high sensitivity.

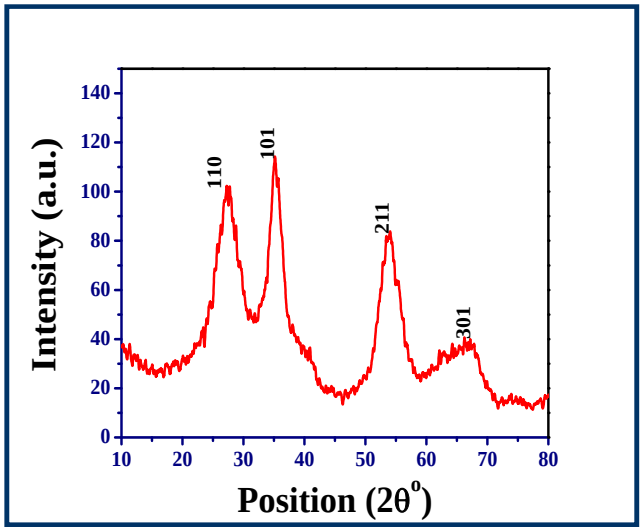

Fig. 3. XRD pattern of $FeSbO_4$.

X-ray diffraction (XRD) analysis

The XRD pattern of the synthesized material prepared after annealing at 450ºC in the presence of 20% oxygen was recorded using an X-ray diffractometer (X-Pert PRO PANalytical) using Cu-K_α radiation (λ = 1.5418 Å) and the pattern is shown in **Fig. 3**. All the diffraction peaks were identified and indexed from the known patterns of standard powder X-ray diffraction data. The synthesized material exhibits four diffraction peaks in (110), (101), (211) and (301) planes. No peaks of single phase α-Fe_2O_3 or Sb_2O_3 were observed. Thus XRD pattern reveals the formation of $FeSbO_4$ compound. This means that $FeSbO_4$ obtained by co-precipitation method might be due to the strong contact between antimony and iron atoms and the possibly high diffusion rate. The XRD reflections assigned to the $FeSbO_4$ appear too broad. The crystallites of $FeSbO_4$ laid in the range 2-4 nm, estimated by employing Debye-Scherrer's formula. The sample has tetragonal crystal structure. The calculated lattice parameters were a = b = 4.5820 Å and c = 3.0854 Å. These tally quite well with the lattice parameters of iron-antimonate given in JCPDS data card (a = b = 4.6351 Å and c = 3.0734 Å). This shows that the material formed consists of tetragonal $FeSbO_4$ lattice structure.

UV-visible absorption spectroscopy

Optical characterization of the sample was done by using UV-visible spectrophotometer (Varian, Carry-50 Bio). **Fig. 4a** presents the variation of optical absorption of the $FeSbO_4$ with the wavelength. A semiconductor exhibits minimal optical absorption for photons with energies smaller than band gap and high absorption for photons with energies greater than the band gap. Consequently, there is a sharp increase in absorption at energies close to the band gap that manifests itself as an absorption edge in the UV-visible absorption spectra. This data was further used for analyzing optical band gap energy (E_g) using the formula for optical absorption of a semiconductor [**43**]:

$$\alpha = \frac{K\left(h\nu - E_g\right)^{n/2}}{h\nu}$$

where 'α' is the absorption coefficient, 'K' is a constant, 'E_g' the optical band gap and 'n' is the number equal to 1 for a direct band gap and 4 for an indirect band gap material. The plot of $(\alpha h\nu)^2$ versus $h\nu$ was used for estimating the value of direct band gap energy of $FeSbO_4$ by extrapolating the linear part of the curve to zero absorption and is shown in **Fig. 4b**. The estimated value of the band gap was found 3.8 eV. The increase of band gap as compared to the bulk can be understood on the basis of quantum size effect [**43**] which arises due to exceptionally small size of nanoparticles.

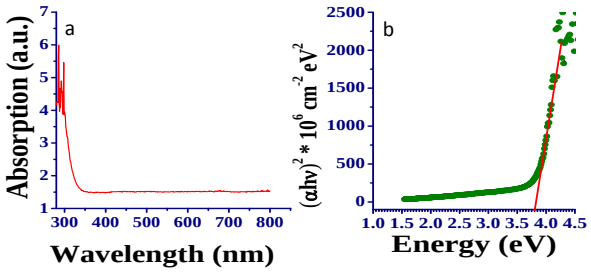

Fig. 4 (a) Absorption as a function of wavelength for $FeSbO_4$, **(b)** Tauc plot for optical band gap.

Results and discussion

Fig. 5a shows the time dependent response of sensing pellet for different vol.% of LPG at room temperature. From figure it is evident that as time increases the resistance of sensing pellet increases drastically in the beginning and then increases linearly. Finally when we open the outlet then the resistance approaches to their initial value of stabilized resistance in air (R_a) for further range of time. Curve '1' of **Fig. 5a** for 1 vol.% of LPG

shows that as time increases the resistance of pellet increases drastically from 10.1 to 18.9 MΩ, after that it increases linearly from 18.9 to 24.5 MΩ with slow response, and finally when we open the outlet the resistance approaches to its initial value of stabilized resistance in air (R_a). Again when we introduced 2 vol.% of LPG resistance increases drastically from 10.1 to 20.3 MΩ, after that it increases linearly from 20.3 to 26.7 MΩ which is shown by curve '2'. This curve shows better slope than previous which indicates the slightly improved sensitivity than previous. Similarly curves '3' and '4' for 3 and 4 vol.% of LPG respectively, shows better slope than previous two's and hence successive improvements in the sensitivities. Finally when we introduced 5 vol.% of LPG, resistance increases drastically from 10.1 to 31.3 MΩ, after that it increases linearly from 31.3 to 36.7 MΩ, which is shown by curve '5'. This is the maximum variation in resistance which gives higher slope and hence highest sensitivity for devising a LPG sensor. As the LPG concentration increases, the sensitivity of sensor increases. The variation of sensitivity with the concentration of LPG is shown in **Fig. 5b** which exhibits linear response for 1-3 vol.% of LPG, after that the sensitivity becomes saturated. The small concentration of gas implies small surface coverage of gas molecules, resulting in a minute surface reaction between the surface adsorbed oxygen species and the gas molecules. The increase in LPG concentration increases the surface reaction due to a large surface coverage. Further on increasing the concentration of LPG, the surface reaction does not increase and eventually saturation takes place. Thus, the maximum sensitivity was obtained at higher concentration of LPG i.e. 5 vol.%. The linearity of sensitivity for the LPG (≤ 3 vol.%) suggests that the $FeSbO_4$ sensing pellet can be reliably used to monitor the LPG over this range of concentration. The maximum sensitivity was 14 MΩ/minute for 5 vol.% of LPG. **Fig. 5c** represents the sensor response curves for the sensing pellets and these curves show that in the beginning, sensor response increases rapidly and later it increases slowly. A variation of average sensor response with LPG concentration is illustrated in **Fig. 5d**. The figure indicates that as the concentration of LPG increases, the average sensor response increases. The maximum average sensor response was 2.2 for 5 vol.% of LPG. High response would be expected if the amount of adsorbed LPG is larger and reaction between the adsorbed LPG and oxygen species is easy. Reproducibility curve for the sensor after one month for 5 vol.% of LPG is plotted and shown in **Fig. 5e**. It shows sensor is 97% reproducible after one month.

Fig. 6a shows that the variations in resistance of $FeSbO_4$ pellet with temperature in the presence of air. In temperature range 100-130°C, the resistance of pellet decreases rapidly and after that it becomes constant, suggesting semi-conducting nature of the pellet. In the lower temperature range $FeSbO_4$ pellet has high resistance. But, with increasing temperature; its resistance became smaller and smaller. In the temperature range 100-250°C, the resistance of $FeSbO_4$ was in the range 423-13 MΩ. **Fig. 6b** shows the Arrhenius plot for iron-antimonate pellet. By measuring the slope of Arrhenius plot of a linear zone, we have calculated the activation energy of $FeSbO_4$ and found 0.92 eV.

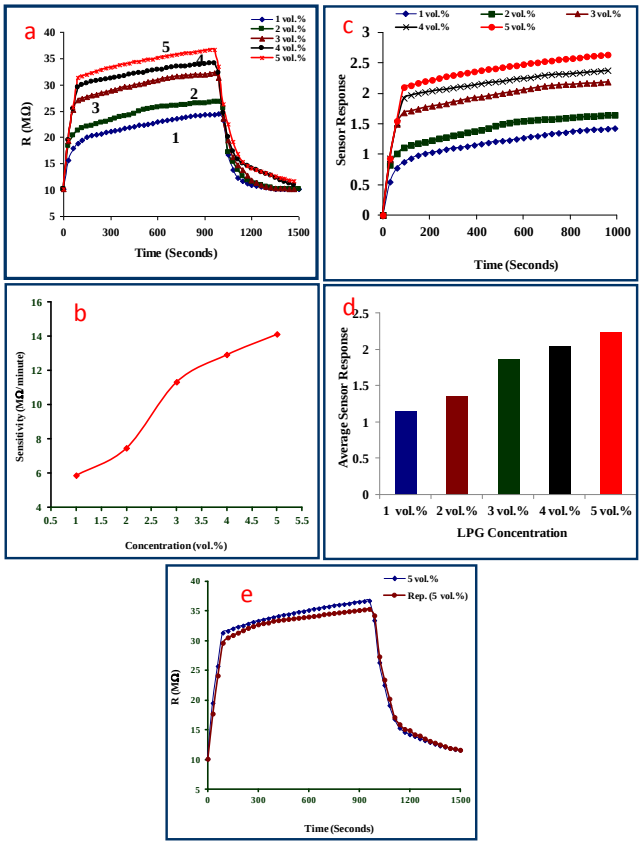

Fig. 5. (a) Variations in resistance of sensing pellet with time for different vol.% of LPG, **5(b)** Sensitivity of sensor with different vol.% of LPG, **5(c)** Sensor response of sensing pellet with time for different vol.% of LPG, **5(d)** Average sensor response of sensing pellet for different vol.% of LPG and **5(e)** Reproducibility curve for sensing pellet after one month.

The temperature-resistance plot in the form of ln R and (1000/T), known as Arrhenius plot, has a slope of (ΔE/2K) according to equation:

$$\ln R = \ln R_0 + \Delta E/2KT$$

where ΔE, K and T are the activation energy, Boltzmann constant and absolute temperature of the material, respectively. The resistance variation of the $FeSbO_4$ with temperature can be described through typical band conduction. It can be noted that a change in temperature will alter the resistance because both the charge of the surface species (O_2, O_2^-, O^- or O^{2-}) as well as their coverage can be altered in this process.

The LPG sensing mechanism of iron-antimonate based LPG sensor is a surface controlled phenomenon i.e., it is based on the surface area of the pellet at which the LPG is adsorbed and reacts with pre-adsorbed oxygen molecules. The oxygen chemisorptions centers viz., oxygen vacancies, localized donor and acceptor states and other defects are formed on the surface during synthesis. These centers are filled by adsorbing oxygen from air. When the sensing pellet is put inside the gas sensing setup then after some time an equilibrium state between oxygen of sensing element and atmospheric oxygen is achieved through the chemisorptions process at room temperature. The stabilized

resistance at present state is known as resistance in presence of air (R_a).

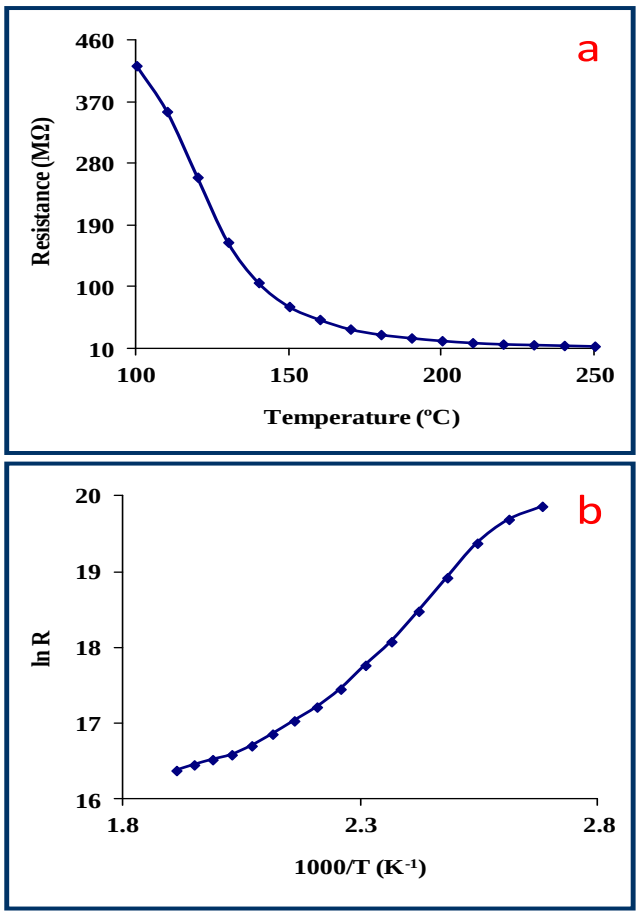

Fig. 6(a). Variation in resistance of pellet with temperature in air and **(b)** Arrhenius plot for iron antimonate pellet.

The reaction kinematics may be explained by the following reactions:

$$O_2(gas) \leftrightarrow O_2(ads).....(i)$$

$$O_2(ads) + e^- \rightarrow O_2^-.....(ii)$$

The electron transfer from the conduction band to the chemisorbed oxygen results in the decrease in the electron concentration at the film surface. As a consequence, an increase in the resistance of the pellet is observed. The conduction process in gas sensing is electronic and the chemisorptions of atmospheric gases take place only at the surface of the sensing elements. Thus, overall conduction in a sensing element, which will monitor the sensor resistance, is determined by the surface reactions resulting from the charge transfer processes with the sensing element. When the pellet is exposed to reducing gas like LPG, it reacts with the chemisorbed oxygen. On interaction with hydrocarbons (C_nH_{2n+2}) of LPG the adsorbed oxygen is removed, forming gaseous species and water vapor. Consequently, the resistance changes, which is due to the change in the width of depletion layer after exposure to LPG. The overall reaction of LPG with the chemisorbed oxygen may takes place as shown below:

$$C_nH_{2n+2} + O_2^- \longrightarrow C_nH_{2n}O + H_2O + e^-$$

where C_nH_{2n+2} represent the various hydrocarbons. When the LPG reacts with the surface oxygen ions then the combustion products such as water depart and a potential barrier to charge transport would be developed i.e., LPG sensing mechanism involves the displacement of adsorbed oxygen species by formation of water. Initially the surface was free from water vapours and pores were dry due to which water vapour adsorbed swiftly. When surface adsorbed water vapours, the condensation of vapour takes place inside the pores and Schottky barrier will form. This potential barrier check to charge carriers and further their transport would not be possible; as a result resistance becomes constant.

Conclusion

The results show that the synthesis process used here gave high yield of $FeSbO_4$ and is proved to be an economical and robust process. The XRD pattern clearly identifies that only tetragonal $FeSbO_4$ phase was formed at 450°C, which inferred proper formation of $FeSbO_4$ compound. The estimated optical band gap of $FeSbO_4$ was 3.8 eV which is significant for gas sensing point of view. The EDAX spectrum confirmed the presence of Sb, Fe and O elements in the sensing material. The maximum sensitivity of $FeSbO_4$ was 14 MΩ/minute for 5 vol.% of LPG. The percentage sensor response was also evaluated and its maximum value was 2.2. The sensing characteristic of the sensor was 97% reproducible after one month, which shows the stability of the fabricated sensor. Thus, this study demonstrates the possibility of utilizing nanostructured $FeSbO_4$ pellet for the detection of LPG at room temperature.

Acknowledgement

The authors acknowledge the support received by the DST Unit on Nanosciences at the Indian Institute of Technology, Kanpur. Mr. Satyendra Singh is thankful to Council of Scientific and Industrial Research (CSIR), India for Senior Research Fellowship vide award no. 09/107(0331)/2008-EMR.

References

1. Jing, Z.; Wang, Y.; Wu, S. *Sens. Actuators B* **2006**, *113*, 177. **DOI**:10.1016/j.snb.2005.02.045
2. Lihua, H.; Qiang, L.; Hui, Z.; Lijun, Y.; Shan, G.; Jinggui, Z. *Sens. Actuators B* **2005,** *107*, 915. **DOI**: 10.1016/j.snb.2004.12.046
3. Rezlescu, N.; Iftimie, N.; Rezlescu, E.; Doroftei, C.; Popa, P.D. *Sens. Actuators B* **2006,** *114*, 427. **DOI**: 10.1016/j.snb.2005.05.030
4. Liu, Y.L.; Wang, H.; Yang, Y.; Liu, Z.M.; Yang, H.F.; Shen, G.L.; Yu, R.Q. *Sens. Actuators B* **2004**, *102*, 148. **DOI**: 10.1016/j.snb.2004.04.014
5. Satyanarayana, L.; Reddy, K.M.; Manorama, S.V. *Mater. Chem. Phys.* **2003**, *82*, 21. **DOI**: 10.1016/S0254-0584 (03)00170-6
6. Xiangfeng, C.; Dongli, J.; Chenmou, Z. *Sens. Actuators B* **2007**, *123*, 793. **DOI:** 10.1016/j.snb.2006.10.020
7. Reddy, K.M.; Satyanarayana, L.; Manorama, S.V.; Mishra, R.D.K. *Mater. Res. Bull.* **2004**, *39*, 1491. **DOI:** 10.1016/j.materresbull.2004.04.022
8. Tan, O.K.; Cao, W.; Zhu, W.; Chai, J.W.; Pan, J.S. *Sens. Actuators B* **2003**, *93*, 396. **DOI:** 10.1016/S0925-4005(03)00191-6
9. Darshane, S.L.; Deshmukh, R.G.; Suryavanshi, S.S.; Mulla, I.S. *J. Am. Ceram. Soc.* **2008**, *91*, 2724. **DOI:** 10.1111/j.1551-2916.2008.02475.x
10. Bang, J.H; Suslick, K.S. *J. Am. Chem. Soc.* **2007**, *129*, 2242.

DOI: 10.1021/ja0676657
11. Zhao, H.; Zhang, Zhigang; Zhao, Zijun; Yu, Ronghua; Wan, Yuanyuan; Lan, Minbo *Advan. Mater. Lett.* **2011**, *2*, 172. **DOI:** 10.5185/amlett.2011.1210
12. Jiang, J.; Yang, Y.M. *Mater. Lett.* **2007**, *61*, 4276. **DOI:** 10.1016/j.matlet.2007.01.111
13. Maensiri, S.; Masingboon, C.; Boonchomb, B.; Seraphin, S. *Scripta Materialia* **2007**, *56*, 797. **DOI:** 10.1016/j.scriptamat.2006.09.033
14. Yue, Z.; Guo, W.; Zhou, J.; Gui, Z.; Li, L. *J. Magn. Magn. Mater.* **2004**, *270*, 216. **DOI:** 10.1016/j.jmmm.2003.08.025
15. Gou, X.; Wang, G.; Park, J.; Liu. H.; Yang, J. *Nanotech.* **2008**, *19*, 125606. **DOI:** 10.1088/0957-4484/19/12/125606
16. Shinde, V.R.; Gujar, T.P.; Lokhande, C.D.; Mane, R.S.; Han, S.H. *Sens. Actuators B* **2007**, *123*, 882. **DOI:** 10.1016/j.snb.2006.10.044
17. Shinde, V.R.; Gujar, T.P.; Lokhande, C.D. *Sens. Actuators B* **2007,** *120*, 551. **DOI:** 10.1016/j.snb.2006.03.007
18. Reddy, C.V.G.; Seela, K.K.; Manorama, S.V. *Inter. J. Inorg. Mater.* **2000**, *2*, 301. **DOI:** 10.1016/S1466-6049 (00)00044-1
19. Vaishampayan, M.V.; Deshmukh, R.G.; Mulla, I.S. *Sens. Actuators B* **2008**, *131*, 665. **DOI:** 10.1016/j.snb.2007.12.055
20. Shinde, V.R.; Gujar, T.P.; Lokhande, C.D. *Sens. Actuators B* **2007**, *123*, 701. **DOI:** 10.1016/j.snb.2006.10.003
21. Comini, E.; Ferroni, M.; Guidi, V.; Faglia, G.; Martinelli, G.; Sberveglieri, G. *Sens. Actuators B* **2002,** *84*, 26. **DOI:** 10.1016/S0925-4005 (02)00006-0
22. Han, J.S.; Davey, D.E.; Mulcahy, D.E.; Yu, A.B. *J. Mater. Sci. Lett.* **1999,** *18*, 975. **DOI:** 10.1023/A:1006671425850
23. Rezlescu, N; Rezlescu, E.; Tudorache, F.; Popa, P.D. *Sens. Trans.* **2007**, *28*, 1134.
24. Liu, Y.L.; Liu, Z.M.; Yang, Y.; Yang, H.F.; Shen, G.L.; Yu, R.Q. *Sens. Actuators B* **2005**, *107*, 600. **DOI:** 10.1016/j.snb.2004.11.026
25. More, A.M.; Gunjakar, J.L.; Lokhande, C.D. *Sens. Actuators B* **2008**, *129*, 671. **DOI:** 10.1016/j.snb.2007.09.026
26. Huang, X.J.; Choi, Y.K. *Sens. Actuators B* **2007**, *122*, 659. **DOI:** 10.1016/j.snb.2006.06.022
27. Crespo, R.G.; Moreira, I.P.R.; Illas, F.; Leeuw, N.H.; Catlow, C.R.A. *J. Mater. Chem.* **2006**, *16*, 1943. **DOI:** 10.1039/b518219k
28. Keulks, G.W.; Lo, M.Y. *J. Phy. Chem.* **1986**, *90*, 4768. **DOI**: 10.1021/j100411a012
29. Rout, C.S.; Krishna, S.H.; Vivekch, S.R.C.; Govindaraj, A.; Rao, C.N.R. *Chem. Phys. Lett.* **2006**, *418*, 586. **DOI**: 10.1016/j.cplett.2005.11.040
30. Barsan, N.; Weimar, U. *J. Phys. Condens. Matter.* **2003**, *15*, R813. **DOI**: 10.1088/0953-8984/15/20/201
31. Dong, L.F.; Cui, J.L.; Zhang, Z.K. *Nano Struc. Mater.* **1997**, *8*, 815. **DOI:** 10.1016/S0965-9773(98)00005-1
32. Xu, Zhikang; Huang, Xiaojun; Wan, Lingshu *Springer* (**2009**).
33. Chang, L.W.; Slikker, William *Neurotoxicology: approaches and methods, academic press*, California, (1995).
34. Tianshu, Z.; Hing, P.; Jiancheng, Z.; Lingbing, K. *Mater. Chem. Phys.* **1999**, *61*, 192.
35. Yadav, B.C.; Srivastava, R.; Yadav, A; Srivastava, V. *Sens. Lett.* **2008**, *6*, 714. **DOI**: 10.1166/sl.2008.m132
36. Yadav, B.C.; Yadav, A.; Shukla, T.; Singh, S. *Sens. Lett.* **2009**, *7*, 1119. **DOI**: 10.1166/sl.2009.1245
37. Yadav, B.C.; Srivastava, R.; Yadav, A. *Sens. Mater.* **2009,** *21*, 87.
38. Yadav, B.C.; Singh, S.; Yadav, A.; Shukla, T. *Int. J. Nanoscience* **2011,** *10*, 135. **DOI**: 10.1142/S0219581X11007478
39. Yadav, B.C.; Singh, S.; Yadav, A. *Appld. Surface Sci.* **2011**, *257*, 1960. **DOI**: 10.1016/j.apsusc.2010.09.035
40. Lagashetty, A.K.; Vijayanand, H.; Basavaraja, S.; Mallikarjuna, N.N.; Venkataraman, A. *Bull Mater. Sci.* **2010**, *33*, 1.
41. Rezlescu, N.; Rezlescu, E.; Tudorache, F.; Popa, P.D. *Roman. Reports Phys.* **2009**, *61* 223.
42. Fischer, P.H.H.; McDowell, C.A. *Can. J. Chem.* **1960**, *38*, 187. **DOI:** 10.1139/v60-025
43. Singh, D.P.; Singh, J.; Mishra, P.R.; Tiwari, R.S.; Srivastava, O.N. *Bull. Mater. Sci.* **2008,** *31*, 319.

